On the importance of fibre direction mesh alignment for artificial lightning strike simulations

B. Nagavel*, S.L.J. Millen and A. Murphy

* School of Mechanical and Aerospace Engineering, Queen's University Belfast, Ashby Building, Belfast, Northern Ireland, U.K., BT9 5AH
e-mail: bnagavel01@qub.ac.uk, web page: pure.qub.ac.uk/en/persons/baskaran-nagavel

ABSTRACT

Composite materials, used in primary aircraft structures, produce weight reduction and improved fuel efficiency over legacy metal airframes but are more susceptible to lightning strike damage. Therefore, research into lightning strike damage and protection systems, through experiments and simulations, is an important research topic. For any FE simulation appropriate representation of the material behaviour, the loading and boundary conditions are key to accurate predictions. In addition, an aspect which has been under reported in many studies is the meshing strategy.

Fibre direction mesh alignment has been reported to yield more accurate results in the modelling of mechanical damage (intralaminar damage initiation and propagation) in unidirectional fibre reinforced composite structures. However, this model meshing strategy has not found wide application and has not been used for the modelling of thermal damage events, e.g. lightning strike direct effect simulation. Instead, authors have typically refined the mesh around the arc attachment area.

This paper, for the first time, examines the influence of fibre direction mesh alignment for artificial lightning strike simulations and the prediction of thermal damage. Initially, the mesh alignment is introduced partially in the central region of the specimen. The paper uses a mature modelling approach with a transient, fully coupled, thermal-electric step in ABAQUS with a lightning test Waveform A (40 kA, 4/20 μs) applied to the specimen. Specimen boundary conditions match those typically used in experiments and a mesh convergence study is undertaken to ensure no element size influence on the results.

The use of this meshing strategy has been shown to significantly improve the prediction of both moderate and severe thermal damage profiles, when compared with the standard meshes used in previous research. The predicted moderate (2659 mm^2 vs 2833 mm^2) and severe (1059 mm^2 vs 1061 mm^2) damage areas were improved to within 4% and 1% of experimental results, respectively, using this meshing strategy.

INTRODUCTION

Composite materials, used in primary aircraft structures, produce weight reduction and improved fuel efficiency over legacy metal airframes but are more susceptible to lightning strike damage. Therefore, research into lightning strike damage and protection systems, through experiments and simulations, is an important research topic. Lightning strikes have been standardised into four discrete waveforms, A-D, presented in SAE-ARP5412B with unique time periods and peak current profiles, used for both simulation and experimental research [1]. The vast majority of simulation studies in the literature have considered Waveform A, which is a 200kA peak current and represents the first return stroke.

Finite element (FE) simulation is the primary approach used to simulate lightning damage of composite material. FE is often used along with more costly experimental analyses as it enables greater insight on the internal damage behaviour and the effective study and control on test and material parameters. For any FE simulation appropriate representation of the material behaviour, the loading and boundary conditions are key to accurate predictions. In addition, an aspect which has been under reported in many

studies is the meshing strategy. Generally, FE meshes are oriented with reference to either the specimen boundaries or to the load introduction. Meshes are often structured, where the element size is refined around the area of interest (where damage is expected) and are courser towards the specimen boundaries. Such meshes have been used throughout literature for many simulation types [2,3]. However, other works have used circular specimens with swept meshes and hex elements or by using o-grid and mid-point subdivision methods [3–7].

Regardless of the aforementioned meshing methods, the alignment of the fibre within the lamina is independent of the mesh. That is to say that the mesh orientation and fibre orientation can be different. An alternative strategy, which has not been employed is to align the mesh based on the ply fibre directions. Fibre aligned meshes are now finding application within composite damage models [8–12] but have thus far been confined to mechanical analyses. This meshing strategy has not been investigated for other simulation types, such as thermal loading. Therefore, this work will assess the effects of fibre aligned meshing for thermal-electric modelling of simulated lightning strikes.

BACKGROUND

Lightning strike experiments

A sizeable amount of experimental research has been conducted on lightning strike damage in a laboratory environment and has typically focussed on the high peak current Waveforms A or D [13–20]. Authors have studied the influence of novel protection systems [13,15–18], paint layers [20], specimen fasteners [21,22] or sequential strikes using multiple waveforms [23–25]. Hirano et al. [19] presented the most complete set of lightning strike damage profiles and these have been used for model validation in literature. Foster et al. [26] used the results from [19] to define two descriptors for the specimen damage due to a strike. Moderate damage was defined as a broad surface region of shiny resin, fibre fracture, matrix cracking, delamination and fibre blow out. Severe damage was defined as a finite, deep region with char residue, fibre fracture and fibre blow out.

Lightning strike simulations and meshing strategies

Complimenting experimental research are lightning strike simulations with the primary focus of these models on the thermal-electric effect in the specimen due to resistive heating [7,24,26–28]. Other works have focussed on pressure loading [29,30], thermal expansion [31,32] or the combination of all physics [33,34].

Thermal-electric models have developed incrementally over a number of years with works focussing on the material system [26,28], boundary conditions [2,26,32,35] and loading [7,26]. The majority of works have focussed on scaled Waveform A with some more recent works focussing on multiple or sequential waveforms applied to the specimen [24,35,36].

Authors have used different methods to generate their FE meshes for thermal-damage models. Some works have used limited refinement around the arc attachment area [37]. Structured meshes, those with refined loading areas, have been used more recently [7,26,28], while radial meshes have also been used [7]. More recently, some authors have reported mesh convergence studies [7,26].

As noted in the introduction the alignment of the fibre within the lamina has until now been independent of the mesh. An alternative strategy is to employ fibre direction mesh alignment. Fibre direction mesh alignment can be achieved in multiple ways but the most common is the use of diamond shaped elements [8,10], allowing the alignment of nodes through the thickness of the specimen, or rotation of square elements by the angle of the fibre orientation [9,11]. A number of works have used fibre aligned meshes for low velocity mechanical impact simulations [8,10,38].

The following section introduces the methodology to be used herein to compare the effects of specimen aligned meshing against a strategy to use fibre aligned meshing for thermal-electric modelling of simulated lightning strikes.

METHODOLOGY

Thermal-electric damage modelling

The thermal-electric simulations, replicating the specimen dimensions (150 x 100 x 4.704 mm), material (IM600/133, provided in a dataset available from ref. [39]) and layup ($[45/0/-45/90]_{4s}$) of ref. [19] were completed using a transient, fully coupled, thermal-electric step in ABAQUS. Lightning test Waveform A (40 kA, 4/20 μs) was applied to the specimen using arc movement and expansion behaviours from previous work [26]. A zero electrical potential boundary condition was applied to the side and bottom surfaces of the specimen model, as with other works in this field [7,26–28,40,41]. Interlaminar thermal and electrical conductivity were included by means of surface-to-surface contact. In all analyses DC3D8E elements were used [42].

Two test cases were compared in this work:

- Case-1, used the previously published mesh from ref. [26] which contained 4200 elements per ply (an in-plane mesh seed of 1.5 mm and 2 elements through the thickness of each ply).
- Case-2, used a refined mesh at the centre of the specimen with diamond shaped elements aligned with the ±45º orientation and the same mesh as Case-1 for the 0º/90º plies. This diamond pattern was created by means of part-level partitioning and meshing. Illustrations of the mesh in the centre of the specimen are shown for +45º plies from both models in Figure 1.

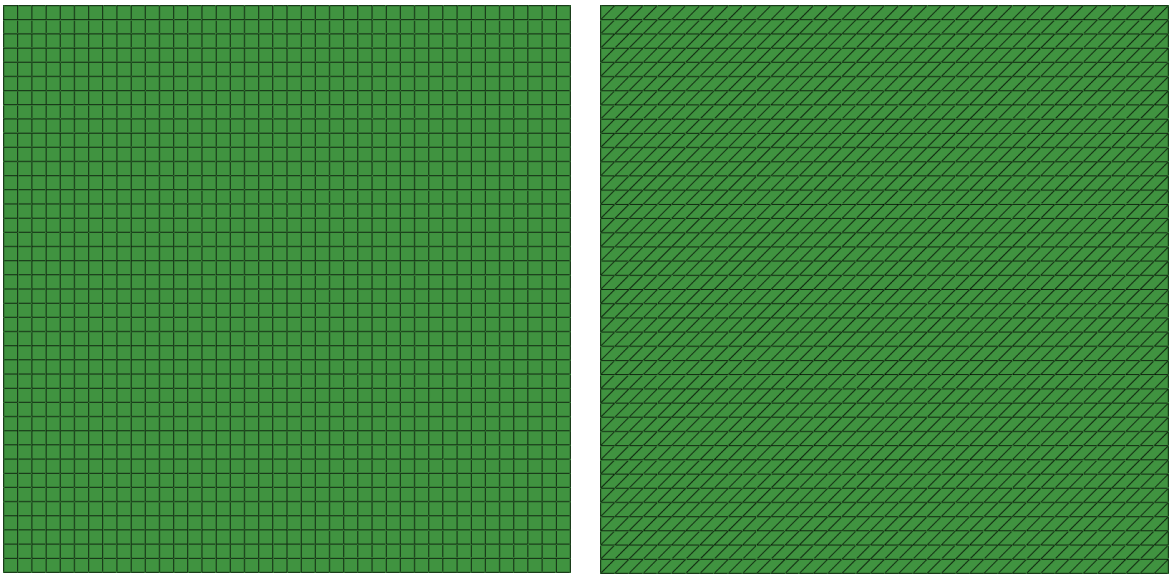

a) Standard refined mesh b) Fibre direction mesh

Figure 1 - FE meshes used in analysis.

A mesh convergence study was conducted on Case-2 following the same procedure as refs. [7,26]. Convergence was assessed by comparing the size of the 300 °C and 500 °C contours on the top surface of the specimen (as these temperatures represent the moderate and severe damage areas and the same method undertaken by refs. [7,26] when converging the baseline case mesh for Case-1). The mesh size was governed by two main criteria; the in-plane mesh size, which corresponded to the size of each diamond and the extent of the refined region.

Initially, the central region was held constant at 30 x 30 mm, shown in Figure 2a, and the diamond size was varied from 1 - 2 mm in 0.5 mm increments. The central region was extended to 50 x 50 mm, shown in Figure 2b, and the diamond size was again varied from 1 - 2 mm in 0.5 mm increments.

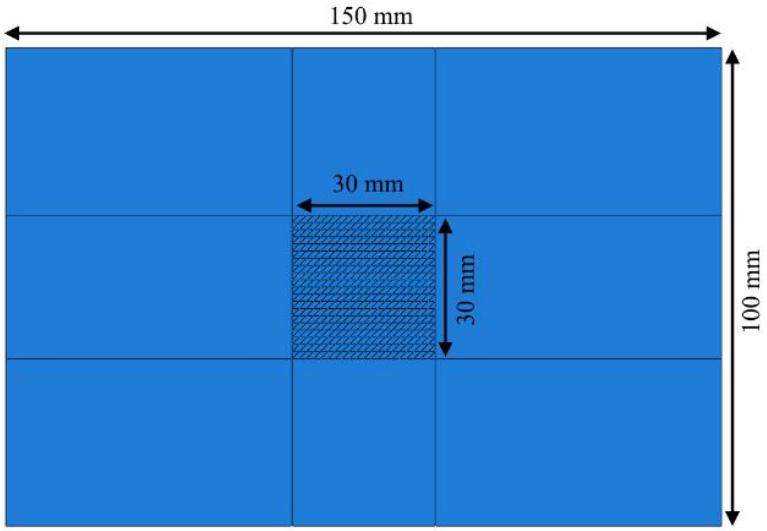

a) 30 x 30 mm central mesh (1.5 mm elements)

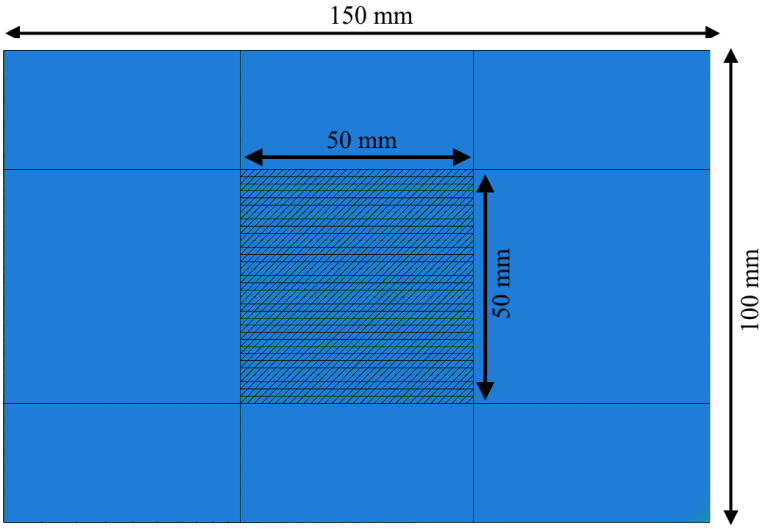

b) 50 x 50 mm central mesh (1.5 mm elements)

Figure 2 - Comparison of central meshes and DoF for 30 x 30 and 50 x 50 cases.

RESULTS

Mesh Convergence for Case-2

Results for the mesh convergence study for Case-2 are presented in Table 1 and shown graphically in Figure 3. Examining Table 1, the mesh convergence study indicates that increasing degrees of freedom, mesh density, progressively increased the size of both the 300°C and the 500°C contours but had less noticeable effect on the damage depth and peak temperature. Moreover, such mesh variation resulted in limited change to the simulation runtime up to Case-2D. Case-2E produced an outlying result for the 300°C contour area, however, the area for the 500°C contour matched the expected trend. Comparing Case-2D and Case-2F the 300 °C contour increases by 3% while the 500 °C contour increases by 9%. However, the increase in runtime was much more pronounced increasing by around 150%.

Due to the large run-time of Case-2F (>5 days), the outlying result for the 300 °C contour from Case-2E and the comparable run-time and element count (4220 per ply) with Case-1, ref. [26] (4200 per ply), the mesh was considered to be converged in Case-2D. Results comparing the effect of mesh orientation, using Case-1 and Case-2D will now be discussed.

Table 1 - Mesh convergence results for Case 2 thermal-electric simulation.

Simulation	Mesh Description	DoF	300°C Contour Area (mm^2)	500°C Contour Area (mm^2)	Depth (plies)	Peak Temp. (°C)
Case-2A	50x50 – 2.0mm	148,390	2552	809	6	980
Case-2B	50x50 – 1.5mm	212,102	2519	898	7	1018
Case-2C	30x30 – 2.0mm	273,922	2690	959	7	1127
Case-2D	30x30 – 1.5mm	372,130	2959	1059	8	1028
Case-2E	50x50 – 1.0mm	384,890	2523	1068	8	1009
Case-2F	30x30 – 1.0mm	653,906	3039	1142	8	1018

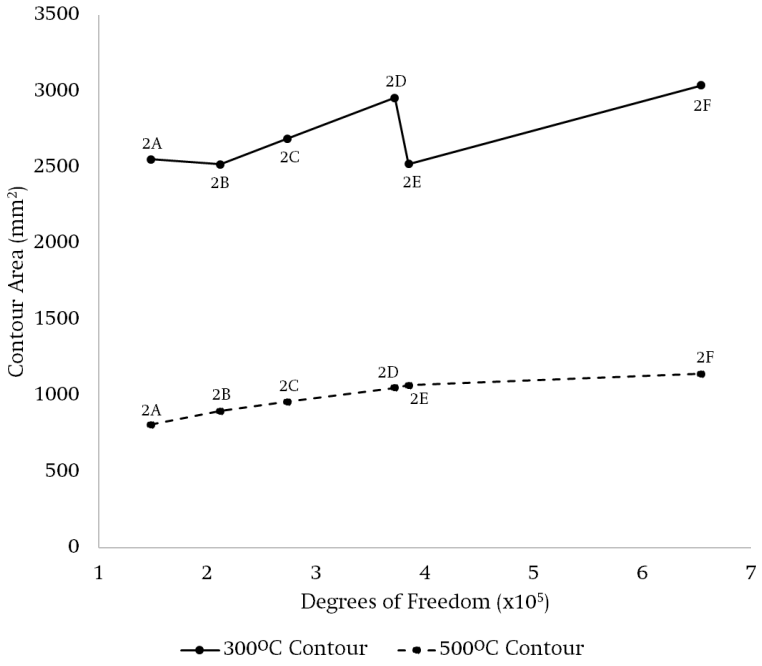

Figure 3 - Case 2 mesh convergence plots.

Thermal-electric results between meshes

Thermal-electric results for the standard mesh (Case-1) and the converged, fibre-aligned mesh (Case-2D) simulations are shown in Figure 4. It can be seen that the fibre-aligned mesh produced much more accurate surface contour predictions when compared with the standard mesh. Visually, the contours now better match the shape of those from the experimental analysis, ref. [19]. The 300°C contour narrows toward both long edges of the specimen using the fibre-aligned mesh, rather than one side for the standard mesh. The 500°C contour, using the fibre-aligned mesh, also produced a damage pattern very close to that of the experiment, in terms of shape and size.

Indeed, comparing the predictions given in Table 2, it can be seen that the use of a fibre-aligned mesh significantly improves predictions. Values for the moderate and severe damage areas were within ±4% and ±1% of the experimental results of Hirano et al. [19], respectively. While the standard mesh overpredicted the moderate damage area by 28% and underpredicted the severe damage area by 8%.

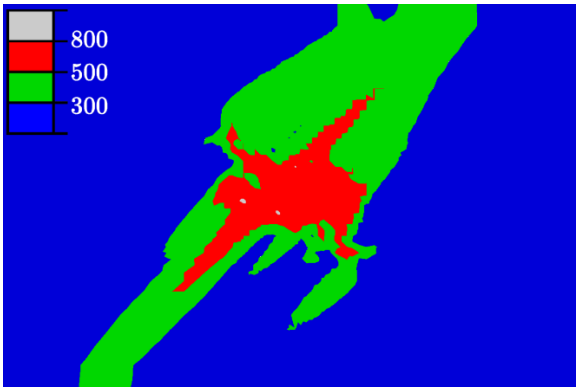

a) Initial mesh

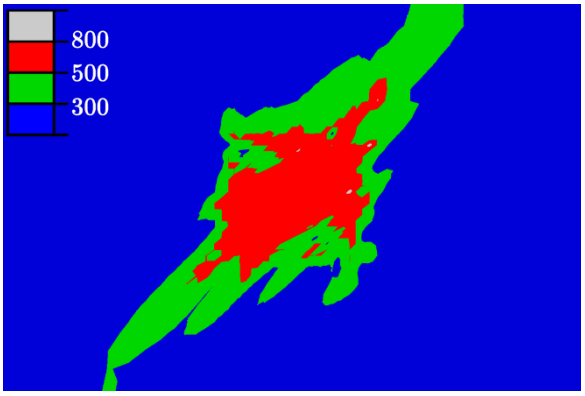

b) Aligned mesh

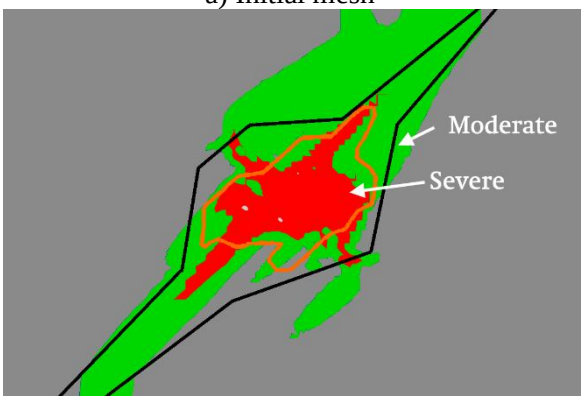

c) Damage outlines - Initial mesh

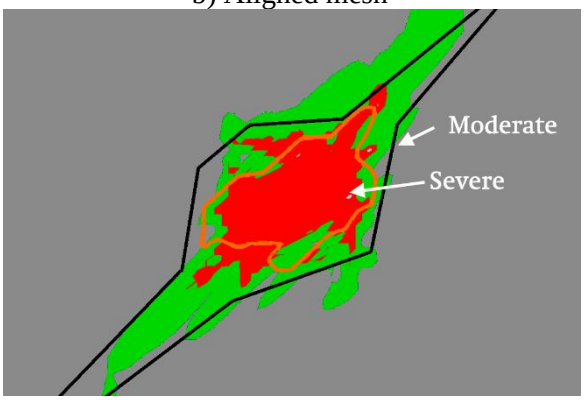

d) Damage outlines - Aligned mesh

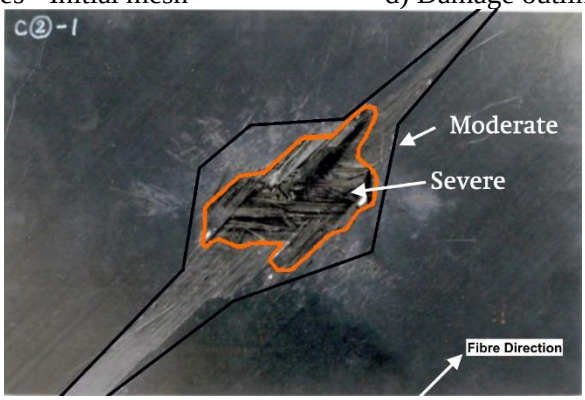

e) Damage outlines on experimental specimen

Figure 4 - Comparison of thermal-damage with and without a fibre aligned mesh.

Table 2 - Damage results summary

Model	Moderate Damage Area (mm^2)	Severe Damage Area (mm^2)	Damage Depth (plies/mm)	Peak Temperature (^oC)
Hirano et al. [19]	2833	1061	8 / 1.1	-
Foster et al., Case 9 [26]	3649	975	7 / 1.029	1089
Fibre Aligned Mesh	2959	1059	8 / 1.176	1028

CONCLUSIONS

The work in this paper has, for the first time, demonstrated the influence of fibre mesh alignment on thermal damage predictions for lightning strike simulations of unidirectional fibre reinforced composites. A mesh convergence study has been completed to show that equivalent standard and fibre-aligned meshes with similar element counts can be directly compared. The use of this meshing strategy has been shown to significantly improve the prediction of both moderate and severe thermal damage profiles, when compared with the standard meshes used in previous research. Predictions of moderate and severe thermal damage were within 4% and 1% of experimental results, respectively.

REFERENCES

[1] SAE Aerospace. Aerospace Recommended Practice ARP5412B. vol. 4970. 1999.

[2] Millen SLJ, Murphy A. Understanding the influence of test specimen boundary conditions on material failure resulting from artificial lightning strike. Eng Fail Anal 2020;114. https://doi.org/10.1016/j.engfailanal.2020.104577.

[3] de Moura MFSF, Gonçalves JPM. Modelling the interaction between matrix cracking and delamination in carbon-epoxy laminates under low velocity impact. Compos Sci Technol 2004;64:1021–7. https://doi.org/10.1016/j.compscitech.2003.08.008.

[4] Armstrong CG, Fogg HJ, Tierney CM, Robinson TT. Common themes in multi-block structured quad/hex mesh generation. Procedia Eng 2015;124:70–82. https://doi.org/10.1016/j.proeng.2015.10.123.

[5] Li TS, McKeag RM, Armstrong CG. Hexahedral meshing using midpoint subdivision and integer programming. Comput Methods Appl Mech Eng 1995;124:171–93. https://doi.org/10.1016/0045-7825(94)00758-F.

[6] Weatherill N, Forsey C. Grid generation and flow calculations for aircraft geometries. J Aircr 1985;22:1985. https://doi.org/10.2514/3.45215.

[7] Millen SLJ, Murphy A, Abdelal G, Catalanotti G. Sequential finite element modelling of lightning arc plasma and composite specimen thermal-electric damage. Comput Struct 2019;222:48–62. https://doi.org/10.1016/j.compstruc.2019.06.005.

[8] Lopes CS, Sádaba S, González C, Llorca J, Camanho PP. Physically-sound simulation of low-velocity impact on fiber reinforced laminates. Int J Impact Eng 2016;92:3–17. https://doi.org/10.1016/j.ijimpeng.2015.05.014.

[9] Laux T, Wui Gan K, Tavares RP, Furtado C, Arteiro A, Camanho PP, et al. Modelling damage in multidirectional laminates subjected to multi-axial loading: ply thickness effects and model assessment. Compos Struct 2021;266:113766. https://doi.org/10.1016/j.compstruct.2021.113766.

[10] González E V., Maimí P, Martín-Santos E, Soto A, Cruz P, Martín de la Escalera F, et al. Simulating drop-weight impact and compression after impact tests on composite laminates using conventional shell finite elements. Int J Solids Struct 2018;144–145:230–47. https://doi.org/10.1016/j.ijsolstr.2018.05.005.

[11] Falcó O, Ávila RL, Tijs B, Lopes CS. Modelling and simulation methodology for unidirectional composite laminates in a Virtual Test Lab framework. Compos Struct 2018;190:137–59. https://doi.org/10.1016/j.compstruct.2018.02.016.

[12] Millen SLJ, Ullah Z, Falzon BG. On the importance of finite element mesh alignment along the fibre direction for modelling damage in fibre-reinforced polymer composite laminates. Compos Struct 2021;278. https://doi.org/10.1016/j.compstruct.2021.114694.

[13] Zhang J, Zhang X, Cheng X, Hei Y, Xing L, Li Z. Lightning strike damage on the composite laminates with carbon nanotube films: Protection effect and damage mechanism. Compos Part B Eng 2019;168:342–52. https://doi.org/10.1016/j.compositesb.2019.03.054.

[14] Xu X, Millen SLJ, Lee J, Abdelal GF, Mitchard D, Wisnom MR, et al. Developing Test Methods for Compression after Lightning Strikes. Appl Compos Mater 2023. https://doi.org/10.1007/s10443-022-10100-w.

[15] Xia Q, Zhang Z, Mei H, Liu Y, Leng J. A double-layered composite for lightning strike protection via conductive and thermal protection. Compos Commun 2020;21. https://doi.org/10.1016/j.coco.2020.100403.

[16] Kumar V, Yokozeki T, Okada T, Hirano Y, Goto T, Takahashi T, et al. Effect of through-thickness electrical conductivity of CFRPs on lightning strike damages. Compos Part A Appl Sci Manuf 2018;114:429–38. https://doi.org/10.1016/j.compositesa.2018.09.007.

[17] Kumar V, Yokozeki T, Karch C, Hassen AA, Hershey CJ, Kim S, et al. Factors affecting direct lightning strike damage to fiber reinforced composites: A review. Compos Part B Eng 2020;183:107688. https://doi.org/10.1016/j.compositesb.2019.107688.

[18] Hirano Y, Yokozeki T, Ishida Y, Goto T, Takahashi T, Qian D, et al. Lightning damage suppression in a carbon fiber-reinforced polymer with a polyaniline-based conductive thermoset matrix. Compos Sci Technol 2016;127:1–7. https://doi.org/10.1016/j.compscitech.2016.02.022.

[19] Hirano Y, Katsumata S, Iwahori Y, Todoroki A. Artificial lightning testing on graphite/epoxy composite laminate. Compos Part A Appl Sci Manuf 2010;41:1461–70. https://doi.org/10.1016/j.compositesa.2010.06.008.

[20] Bigand A, Espinosa C, Bauchire JM. Equivalent mechanical load model methodology to simulate lightning strike impact on protected and painted composite structure. Compos Struct 2022;280. https://doi.org/10.1016/j.compstruct.2021.114886.

[21] Feraboli P, Miller M. Damage resistance and tolerance of carbon/epoxy composite coupons subjected to simulated lightning strike. Compos Part A Appl Sci Manuf 2009;40:954–67. https://doi.org/10.1016/j.compositesa.2009.04.025.

[22] Feraboli P, Kawakami H. Damage of Carbon/Epoxy Composite Plates Subjected to Mechanical Impact and Simulated Lightning. J Aircr 2010;47:999–1012. https://doi.org/10.2514/1.46486.

[23] Sun J, Yao X, Tian X, Chen J, Wu Y. Damage Characteristics of CFRP Laminates Subjected to Multiple Lightning Current Strike. Appl Compos Mater 2018;26:745–762. https://doi.org/10.1007/s10443-018-9747-4.

[24] Dong Q, Wan G, Guo Y, Zhang L, Wei X, Yi X, et al. Damage analysis of carbon fiber composites exposed to combined lightning current components D and C. Compos Sci Technol 2019;179:1–9. https://doi.org/10.1016/j.compscitech.2019.04.030.

[25] Sun J, Yao X, Xu W, Chen J, Wu Y. Evaluation method for lightning damage of carbon fiber reinforced polymers subjected to multiple lightning strikes with different combinations of current components. J Compos Mater 2020;54:111–25. https://doi.org/10.1177/0021998319860562.

[26] Foster P, Abdelal G, Murphy A. Understanding how arc attachment behaviour influences the prediction of composite specimen thermal loading during an artificial lightning strike test. Compos Struct 2018;192:671–83. https://doi.org/10.1016/j.compstruct.2018.03.039.

[27] Millen SLJ, Murphy A, Abdelal G, Catalanotti G. Specimen Representation on the Prediction of Artificial Test Lightning Plasma, Resulting Specimen Loading and Subsequent Composite

Material Damage. Compos Struct 2020;231:111545. https://doi.org/10.1016/j.compstruct.2019.111545.

[28] Chen H, Wang FS, Ma XT, Yue ZF. The coupling mechanism and damage prediction of carbon fiber/epoxy composites exposed to lightning current. Compos Struct 2018;203:436–45. https://doi.org/10.1016/j.compstruct.2018.07.017.

[29] Karch C, Arteiro A, Camanho PP. Modelling mechanical lightning loads in carbon fibre-reinforced polymers. Int J Solids Struct 2018;162:217–43. https://doi.org/10.1016/j.ijsolstr.2018.12.013.

[30] Foster P, Abdelal G, Murphy A. Quantifying the Influence of Lightning Strike Pressure Loading on Composite Specimen Damage. Appl Compos Mater 2018;26:115–37. https://doi.org/10.1007/s10443-018-9685-1.

[31] Foster P, Abdelal G, Murphy A. Modelling of mechanical failure due to constrained thermal expansion at the lightning arc attachment point in carbon fibre epoxy composite material. Eng Fail Anal 2018;94:364–78. https://doi.org/10.1016/j.engfailanal.2018.08.003.

[32] Dong Q, Wan G, Ping L, Guo Y, Yi X, Jia Y. Coupled thermal-mechanical damage model of laminated carbon fiber/resin composite subjected to lightning strike. Compos Struct 2018;206:185–93. https://doi.org/10.1016/j.compstruct.2018.08.043.

[33] Millen SLJ, Murphy A, Catalanotti G, Abdelal G. Coupled thermal-mechanical progressive damage model with strain and heating rate effects for lightning strike damage assessment. Appl Compos Mater 2019;26:1437–59. https://doi.org/10.1007/s10443-019-09789-z.

[34] Harrell TM, Madsen SF, Thomsen OT, Dulieu-Barton JM. On the Effect of Dielectric Breakdown in UD CFRPs Subjected to Lightning Strike Using an Experimentally Validated Model. Appl Compos Mater 2022. https://doi.org/10.1007/s10443-022-10014-7.

[35] Wang FS, Zhang Y, Ma XT, Wei Z, Gao JF. Lightning ablation suppression of aircraft carbon/epoxy composite laminates by metal mesh. J Mater Sci Technol 2019;35:2693–704. https://doi.org/10.1016/j.jmst.2019.07.010.

[36] Wan G, Dong Q, Zhi J, Guo Y, Yi X, Jia Y. Analysis on electrical and thermal conduction of carbon fiber composites under lightning based on electrical-thermal-chemical coupling and arc heating models. Compos Struct 2019;229:111486. https://doi.org/10.1016/j.compstruct.2019.111486.

[37] Shah SZH, Lee J. Stochastic lightning damage prediction of carbon/epoxy composites with material uncertainties. Compos Struct 2022;282. https://doi.org/10.1016/j.compstruct.2021.115014.

[38] Sádaba S, Martínez-Hergueta F, Lopes CS, Gonzalez C, LLorca J. Virtual testing of impact in fiber reinforced laminates. In: Beaumont PWR, Soutis C, Hodzic A, editors. Struct. Integr. Durab. Adv. Compos., Woodhead Publishing; 2015, p. 247–70. https://doi.org/10.1017/S0030605311001384.

[39] Millen SLJ, Murphy A. Spatial and temporal Waveform A and B loading and material data for lightning strike simulations based on converged FE Meshes 2021. https://doi.org/10.17034/ef3ff864-78d3-4ce4-9c0f-fec7b4c408a0.

[40] Ogasawara T, Hirano Y, Yoshimura A. Coupled thermal-electrical analysis for carbon fiber/epoxy composites exposed to simulated lightning current. Compos Part A Appl Sci Manuf 2010;41:973–81. https://doi.org/10.1016/j.compositesa.2010.04.001.

[41] Abdelal GF, Murphy A. Nonlinear numerical modelling of lightning strike effect on composite panels with temperature dependent material properties. Compos Struct 2014;109:268–78. https://doi.org/10.1016/j.compstruct.2013.11.007.

[42] ABAQUS 2016 Documentation. ABAQUS Theory Manual. 2017.